Error Estimates for the Upwind Discontinuous Galerkin Method on Locally Smooth Meshes and Meshes with Periodic Patterns

Doudou Wang*, Yan Jiang†, Jianfang Lu‡, Chi-Wang Shu§, Mengping Zhang¶, Zhenya Huang‖, and Enhong Chen**

Abstract

We study L^2 error estimates for the semidiscrete upwind discontinuous Galerkin (DG) method applied to the linear transport equation with constant coefficients in two dimensions. The approximation uses P^k elements of total degree on structured nonuniform Cartesian meshes. We identify two mesh structures that retain improved accuracy on nonuniform meshes. For locally smooth meshes, where adjacent cell sizes differ by $O(h^{1+\alpha})$ with $\alpha > \frac{1}{2}$, an elementwise shifted upwind projection gives

$$\|u(T) - u_h(T)\|_{L^2(\Omega)} \leqslant C_T h^{k+\theta}, \qquad \theta = \min\{\alpha, 1\}.$$

For meshes with periodic patterns, where every macro cell repeats the same fixed internal pattern, we introduce a projection on each macro cell. Its exact translation property at the macro scale yields the optimal estimate

$$\|u(T) - u_h(T)\|_{L^2(\Omega)} \leqslant C_T h^{k+1} \|u_0\|_{H^{k+2}(\Omega)}.$$

*School of Mathematical Sciences, University of Science and Technology of China, Hefei, Anhui 230026, China. E-mail: ampmw@mail.ustc.edu.cn.

†School of Mathematical Sciences, University of Science and Technology of China, Hefei, Anhui 230026, China. E-mail: jiangy@ustc.edu.cn. Research is supported by National Natural Science Foundation of China (No. 12271499).

‡School of Mathematics, South China University of Technology, Canton, Guangdong 510641, China. Corresponding author. E-mail: jflu@scut.edu.cn. Research is supported by Guangdong Basic and Applied Basic Research Foundation (No. 2026B1515020064).

§Division of Applied Mathematics, Brown University, Providence, RI 02912, USA. E-mail: chiwang_shu@brown.edu.

¶School of Mathematical Sciences, University of Science and Technology of China, Hefei, Anhui 230026, China. E-mail: mpzhang@ustc.edu.cn.

‖State Key Laboratory of Cognitive Intelligence, University of Science and Technology of China, Hefei, Anhui 230027, China. Corresponding author. E-mail: huangzhy@ustc.edu.cn. Research is supported by Young Elite Scientists Sponsorship Program by CAST (No. 2024QNRC001).

**State Key Laboratory of Cognitive Intelligence, University of Science and Technology of China, Hefei, Anhui 230027, China. E-mail: cheneh@ustc.edu.cn. Research is supported by National Natural Science Foundation of China (No. U23A20319).

Thus local smoothness leads to an approximate shifting argument with a rate depending on α, while pattern periodicity yields the optimal order through translation at the macro scale. Numerical tests confirm both residual mechanisms and the observed convergence of the DG solution. Results for the standard local L^2 projection are included for comparison.

Keywords. Error estimate; discontinuous Galerkin method; shifted projection; locally smooth mesh; Cartesian mesh with a periodic pattern.
MSC. 65M60, 65M15.

1 Introduction

The discontinuous Galerkin (DG) method was first introduced by Reed and Hill [23] for the neutron transport equation, and was subsequently developed into the Runge–Kutta DG (RKDG) framework for nonlinear hyperbolic conservation laws by Cockburn et al. [7, 6, 8, 10]. The mathematical analysis of DG methods can be traced back to LeSaint and Raviart [16], who proved convergence rates of $O(h^k)$ for P^k elements on general triangulations and $O(h^{k+1})$ for Q^k elements on Cartesian grids in the standard L^2 norm. Johnson and Pitkäranta [15] later proved $O(h^{k+1/2})$ in a norm depending on the mesh for P^k elements on general triangulations, and Peterson [22] showed that this rate is optimal. On special grids, Richter [24] obtained the optimal $O(h^{k+1})$ rate, while Cockburn, Dong, and Guzmán [5] proved optimal convergence on simplex meshes satisfying suitable flow conditions. Falk and Richter [12] established $O(h^{k+1/2})$ for Friedrichs systems, and Houston, Schwab, and Süli [14] obtained exponential convergence in an hp analysis for piecewise analytic solutions. The effect of mesh partitioning on elements of low degree was studied in [29, 17]. Optimal $O(h^{k+1})$ estimates are classical in one dimension and for Q^k elements in several dimensions [28]. Fluxes biased toward the upwind direction were studied in [20], and equations of higher order were analyzed in [9, 25].

The case of P^k spaces of total degree on Cartesian meshes in two dimensions is less direct. The space P^k is computationally attractive because its local dimension $\frac{1}{2}(k+1)(k+2)$ is only about half that of Q^k. Numerical evidence also suggests that the rate can improve from $O(h^{k+1/2})$ to $O(h^{k+1})$ on Cartesian grids. However, the moment conditions used for Q^k elements are overdetermined in the smaller P^k space. A different projection is therefore needed to control the interface terms. Liu, Shu, and Zhang [19] resolved this problem for linear equations with constant coefficients on uniform meshes. They used a shifted upwind projection whose orthogonality conditions match the DG bilinear form. The shifting technique was introduced earlier in [18] for central DG methods. Cao, Shu, and Zhang [2] later gave a unified analysis of linear equations with variable coefficients and nonlinear equations on uniform Cartesian meshes. Their correction function technique gives optimal L^2 estimates of order $k+1$ for every $k \geqslant 0$. It also gives $O(h^{k+2})$ superconvergence for the cell average and the downwind edge average. This appears to be the first such result for P^k elements; earlier studies considered one dimension or Q^k elements in several dimensions (see, e.g., [3, 27, 1]). On nonuniform meshes, these errors converge at the optimal rate $O(h^{k+1})$, without superconvergence [2].

The argument of [19] is also restricted to uniform meshes for the basic L^2 estimate. The shifted projection on one cell is tied to the projection on its neighbor by a rigid translation, and this invariance forces the dominant interface mismatch to cancel. On a nonuniform mesh, the translation no longer maps one cell onto the next; the cancellation is lost, and the same reasoning yields only the suboptimal rate h^k. On a general nonuniform mesh satisfying shape regularity, the standard L^2 projection instead gives $O(h^{k+1/2})$ through a trace inequality (see Section 2.4); this matches the rate on general triangulations [15, 22] and is sharp.

These observations suggest that the convergence rate is governed not by nonuniformity alone, but by the remaining structure in the interface projection mismatch. We study two such structures. The first is a local smoothness condition on adjacent cell sizes. Analogous $O(h^{1+\alpha})$ geometric assumptions have appeared in the finite element superconvergence literature: Xu and Zhang [26] used an approximate parallelogram condition to establish $O(h^{1+\rho})$ superconvergence, with $\rho = \min(\alpha, \frac{1}{2}, \frac{\sigma}{2})$, for gradient recovery operators, and Naga and Zhang [21] used the same structure to prove asymptotic exactness of polynomial preserving recovery. In the present Cartesian setting, this condition controls the variation of the cell aspect ratio $\lambda_{i,j} = h_i^x/h_j^y$ across interfaces and supplies the additional factor needed to estimate differences between shifted traces. The second structure is a periodically repeated pattern at the macro scale. The mesh may be nonuniform within each macro cell, and adjacent fine cells may differ by $O(h)$. However, grouping fine cells into macro cells preserves an exact translation property. An upwind projection on each macro cell then cancels the residuals on internal fine interfaces. The remaining differences across macro interfaces provide an additional factor H. Our contribution is a unified analysis of these two mechanisms. On locally smooth meshes, the shifted projection is defined through a reference bilinear form that depends on the aspect ratio. On meshes with periodic patterns, a projection is constructed on each macro cell. Both cases are treated by the same approximation and residual estimates.

The remainder of the paper is organized as follows. Section 2 presents the DG scheme, the common error framework, a baseline estimate, and the main results. Sections 3 and 4 analyze locally smooth meshes and meshes with periodic patterns, respectively. Section 5 reports numerical tests, Section 6 concludes the paper, and the appendix contains the longer technical proofs.

2 The DG scheme and a common error framework

2.1 Model problem and DG scheme

We first recall the general setting for scalar hyperbolic conservation laws and their DG discretization. Let $\Omega \subset \mathbb{R}^d$ be a bounded domain and let $\mathbf{f} = (f_1, \ldots, f_d)$ be a smooth flux function. A general initial-boundary value problem has the form

$$u_t + \nabla \cdot \mathbf{f}(u) = 0, \qquad \mathbf{x} \in \Omega, \quad 0 < t \leqslant T,$$

together with the initial condition $u(\mathbf{x}, 0) = u_0(\mathbf{x})$ and suitable inflow boundary data. On a mesh $\mathcal{T}_h$ of Ω, the DG method seeks an approximation u_h in a broken polynomial space. Multiplying by a test function v_h and integrating the flux term by parts on each cell gives the semidiscrete formulation

$$\sum_{K\in\mathcal{T}_h}\int_K (u_h)_t v_h \,\mathrm{d}\mathbf{x} - \sum_{K\in\mathcal{T}_h}\int_K \mathbf{f}(u_h)\cdot\nabla v_h \,\mathrm{d}\mathbf{x} + \sum_{K\in\mathcal{T}_h}\int_{\partial K}\widehat{f}(u_h^-,u_h^+;\mathbf{n}_K)v_h^- \,\mathrm{d}\sigma = 0,$$

for all test functions v_h in the same broken polynomial space. Here $\mathbf{n}_K$ is the outward unit normal to K, u_h^- and u_h^+ denote the interior and exterior traces on a cell boundary, and $\widehat{f}$ is a consistent numerical normal flux. For a linear transport equation $u_t+\mathbf{b}\cdot\nabla u=0$, the upwind flux uses the trace from the upwind side: $\widehat{f}(u_h^-,u_h^+;\mathbf{n}_K)=(\mathbf{b}\cdot\mathbf{n}_K)u_h^-$ if $\mathbf{b}\cdot\mathbf{n}_K\geqslant 0$, and $\widehat{f}(u_h^-,u_h^+;\mathbf{n}_K)=(\mathbf{b}\cdot\mathbf{n}_K)u_h^+$ otherwise.

We now consider the linear transport equation with constant coefficients in two dimensions. Let $\Omega=[0,L_x]\times[0,L_y]$ be a rectangular domain and consider

$$\begin{cases} u_t+u_x+u_y=0, & (x,y)\in\Omega,\quad 0<t\leqslant T,\\ u(x,y,0)=u_0(x,y), \end{cases} \tag{1}$$

with periodic boundary conditions in both x and y. Let

$$0=x_{\frac12}<x_{\frac32}<\cdots<x_{N_x+\frac12}=L_x,\qquad 0=y_{\frac12}<y_{\frac32}<\cdots<y_{N_y+\frac12}=L_y.$$

Define

$$I_i^x=(x_{i-\frac12},x_{i+\frac12}),\quad I_j^y=(y_{j-\frac12},y_{j+\frac12}),\quad K_{i,j}=I_i^x\times I_j^y,$$

for $1\leqslant i\leqslant N_x$, $1\leqslant j\leqslant N_y$, and

$$h_i^x=x_{i+\frac12}-x_{i-\frac12},\quad h_j^y=y_{j+\frac12}-y_{j-\frac12},\quad x_i=\frac{x_{i-\frac12}+x_{i+\frac12}}{2},\quad y_j=\frac{y_{j-\frac12}+y_{j+\frac12}}{2},$$

with mesh size $h=\max\{\max_i h_i^x,\max_j h_j^y\}$. On $K_{i,j}$ we use the centered reference coordinates

$$x=x_i+h_i^x\xi,\quad y=y_j+h_j^y\eta,\quad (\xi,\eta)\in\widehat{K}:=[-\tfrac12,\tfrac12]^2.$$

Throughout the analysis, the underlying fine mesh is assumed to be quasi-uniform: there exist constants $c_0,C_0>0$ independent of h such that

$$c_0\,h\leqslant h_i^x,\ h_j^y\leqslant C_0\,h. \tag{2}$$

For an integer $k\geqslant 0$, set

$$P^k(K_{i,j}):=\operatorname{span}\{(x-x_i)^\ell(y-y_j)^m : 0\leqslant \ell+m\leqslant k\},$$

and define the semidiscrete DG space

$$V_h^k:=\{v_h\in L^2(\Omega): v_h|_{K_{i,j}}\in P^k(K_{i,j}),\ \forall\, i,j\}.$$

With velocity $\mathbf{b}=(1,1)$, the outflow edges of $K_{i,j}$ are the right edge and the top edge:

$$e_{i,j,+}^x=\{x_{i+\frac12}\}\times I_j^y,\qquad e_{i,j,+}^y=I_i^x\times\{y_{j+\frac12}\}.$$

On a vertical outflow edge $e_{i,j,+}^x$, let v_h^- denote the trace from $K_{i,j}$ and v_h^+ the trace from $K_{i+1,j}$. Define the upwind jump

$$[v_h]_{i,j}^x:=v_h^- - v_h^+.$$

Analogously, on a horizontal outflow edge $e^y_{i,j,+}$, with traces v_h^- from $K_{i,j}$ and v_h^+ from $K_{i,j+1}$,

$$[v_h]^y_{i,j} := v_h^- - v_h^+.$$

For a piecewise smooth function w and any $v_h \in V_h^k$, define

$$\begin{aligned}\mathcal{H}(w, v_h) := &-\sum_{i,j} \int_{K_{i,j}} w\big((v_h)_x + (v_h)_y\big)\, \mathrm{d}x\, \mathrm{d}y \\ &+ \sum_{i,j} \int_{e^x_{i,j,+}} w^- [v_h]^x_{i,j}\, \mathrm{d}\sigma + \sum_{i,j} \int_{e^y_{i,j,+}} w^- [v_h]^y_{i,j}\, \mathrm{d}\sigma.\end{aligned} \tag{3}$$

The semidiscrete upwind DG scheme reads: find $u_h(t) \in V_h^k$ such that

$$((u_h)_t, v_h)_\Omega + \mathcal{H}(u_h, v_h) = 0, \qquad \forall\, v_h \in V_h^k. \tag{4}$$

2.2 Consistency and energy identities

Lemma 2.1 (Consistency)**.** *If w is a globally smooth periodic function, then*

$$\mathcal{H}(w, v_h) = \int_\Omega (w_x + w_y)\, v_h\, \mathrm{d}x\, \mathrm{d}y, \qquad \forall\, v_h \in V_h^k.$$

In particular, choosing $w = u$ and invoking the PDE (1) gives the Galerkin orthogonality

$$\big((u - u_h)_t, v_h\big)_\Omega + \mathcal{H}(u - u_h, v_h) = 0, \qquad \forall\, v_h \in V_h^k. \tag{5}$$

Proof. Integration by parts on each $K_{i,j}$ gives

$$-\int_{K_{i,j}} w\big((v_h)_x + (v_h)_y\big)\, \mathrm{d}x\, \mathrm{d}y = \int_{K_{i,j}} (w_x + w_y) v_h\, \mathrm{d}x\, \mathrm{d}y - \int_{\partial K_{i,j}} w v_h (\mathbf{b} \cdot \mathbf{n})\, \mathrm{d}\sigma.$$

Since w is single-valued across interfaces, the boundary contributions cancel exactly against the upwind jump terms in (3), and the periodic outer boundary is treated identically. Summing over all cells gives the consistency identity. The Galerkin orthogonality (5) then follows by subtracting the scheme (4) from the weak form of the PDE. □

Lemma 2.2 (Upwind energy identity)**.** *For any $v_h \in V_h^k$,*

$$\mathcal{H}(v_h, v_h) = J_h(v_h)^2, \tag{6}$$

where

$$J_h(v_h)^2 := \frac{1}{2} \sum_{i,j} \left(\int_{e^x_{i,j,+}} \big([v_h]^x_{i,j}\big)^2 \mathrm{d}\sigma + \int_{e^y_{i,j,+}} \big([v_h]^y_{i,j}\big)^2 \mathrm{d}\sigma \right) \geqslant 0.$$

Proof. On each cell, $-\int_{K_{i,j}} v_h((v_h)_x + (v_h)_y) = -\frac{1}{2} \int_{K_{i,j}} \big(\partial_x(v_h^2) + \partial_y(v_h^2)\big)$. On a vertical interface with traces $a = v_h^-$ and $b = v_h^+$, the volume term contributes $-\frac{1}{2}a^2 + \frac{1}{2}b^2$ and the upwind flux contributes $a(a-b)$; their sum is $\frac{1}{2}(a-b)^2$. Summing over all periodic interfaces gives (6). □

2.3 A common framework based on projection errors

The two mesh analyses below share the same energy argument. Let Π_h be a linear projection into V_h^k that is independent of time, and set $\rho = u - \Pi_h u$. Suppose that, for some $s > 0$ and some regularity measure M_T,

$$\|\rho(t)\|_{L^2(\Omega)} + \|\rho_t(t)\|_{L^2(\Omega)} \leqslant C h^s M_T, \qquad 0 \leqslant t \leqslant T, \tag{7}$$

and

$$|\mathcal{H}(\rho(t), v_h)| \leqslant C h^s M_T \|v_h\|_{L^2(\Omega)}, \qquad \forall\, v_h \in V_h^k. \tag{8}$$

Then the following estimate follows immediately from Lemmas 2.1 and 2.2.

Proposition 2.3 (Abstract estimate based on projection errors)**.** *Let u be the periodic solution of* (1)*, and let u_h solve* (4)*. If Π_h satisfies* (7)–(8)*, then*

$$\|u(T) - u_h(T)\|_{L^2(\Omega)} \leqslant C_T\big(\|\Pi_h u(0) - u_h(0)\|_{L^2(\Omega)} + h^s M_T\big).$$

Proof. Write $u - u_h = \rho + \xi_h$ with $\xi_h = \Pi_h u - u_h$. Galerkin orthogonality gives

$$((\xi_h)_t, v_h)_\Omega + \mathcal{H}(\xi_h, v_h) = -(\rho_t, v_h)_\Omega - \mathcal{H}(\rho, v_h).$$

Taking $v_h = \xi_h$, using Lemma 2.2, and applying (7)–(8) gives

$$\frac{1}{2}\frac{\mathrm{d}}{\mathrm{d}t}\|\xi_h\|^2_{L^2(\Omega)} \leqslant C h^s M_T \|\xi_h\|_{L^2(\Omega)}.$$

A standard regularization argument for the case $\|\xi_h\|_{L^2(\Omega)} = 0$, followed by integration in time, yields

$$\|\xi_h(T)\|_{L^2(\Omega)} \leqslant \|\xi_h(0)\|_{L^2(\Omega)} + C_T h^s M_T.$$

The estimate follows from $\|u(T) - u_h(T)\|_{L^2(\Omega)} \leqslant \|\rho(T)\|_{L^2(\Omega)} + \|\xi_h(T)\|_{L^2(\Omega)}$ and (7). □

2.4 A baseline estimate with the standard L^2 projection

Let $\mathbb{P}_h$ denote the standard elementwise L^2 projection, defined by

$$\int_{K_{i,j}} (\mathbb{P}_h w - w)\, v_h \,\mathrm{d}x\,\mathrm{d}y = 0, \qquad \forall\, v_h \in P^k(K_{i,j}),$$

This projection gives the rate $h^{k+1/2}$ on general nonuniform meshes. By standard approximation theory [4],

$$\|u - \mathbb{P}_h u\|_{L^2(\Omega)} \leqslant C h^{k+1} \|u\|_{H^{k+1}(\Omega)}. \tag{9}$$

Proposition 2.4 (Suboptimal L^2 estimate with $\mathbb{P}_h$)**.** *Let u be the periodic solution of* (1) *with $u \in L^\infty(0,T;H^{k+2}(\Omega)) \cap C^1([0,T];H^{k+1}(\Omega))$. Let $u_h(t) \in V_h^k$ be the semidiscrete upwind DG solution of* (4)*, initialized by $u_h(0) = \mathbb{P}_h u(0)$. Assume that the mesh satisfies* (2)*. Then*

$$\|u(T) - u_h(T)\|_{L^2(\Omega)} \leqslant C_T\, h^{k+\frac{1}{2}}\, \widetilde{M}_T,$$

where $\widetilde{M}_T := \sup_{0\leqslant t\leqslant T}\big(\|u(t)\|_{H^{k+1}(\Omega)} + \|u_t(t)\|_{H^{k+1}(\Omega)}\big)$.

Proof. Decompose the error as $e = u - u_h = \eta + \xi_h$, where $\eta = u - \mathbb{P}_h u$ and $\xi_h = \mathbb{P}_h u - u_h \in V_h^k$. By Lemmas 2.1 and 2.2,

$$\tfrac{1}{2}\tfrac{\mathrm{d}}{\mathrm{d}t}\left\|\xi_h\right\|_{L^2(\Omega)}^2 + J_h(\xi_h)^2 = -(\eta_t, \xi_h)_\Omega - \mathcal{H}(\eta, \xi_h).$$

The L^2 orthogonality of η eliminates the volume integrals in $\mathcal{H}(\eta, \xi_h)$, leaving only the interface traces:

$$\mathcal{H}(\eta, \xi_h) = -\sum_{i,j}\int_{I_j^y} \eta_{i+\frac{1}{2}}^- [\xi_h]_{i,j}^x \,\mathrm{d}y - \sum_{i,j}\int_{I_i^x} \eta_{j+\frac{1}{2}}^- [\xi_h]_{i,j}^y \,\mathrm{d}x.$$

Applying Cauchy–Schwarz and the multiplicative trace inequality on each $K_{i,j}$,

$$\left\|\eta_{i+\frac{1}{2}}^-\right\|_{L^2(I_j^y)}^2 \leqslant C\big((h_i^x)^{-1}\left\|\eta\right\|_{L^2(K_{i,j})}^2 + h_i^x \left\|\nabla\eta\right\|_{L^2(K_{i,j})}^2\big),$$

and summing with quasi-uniformity and (9) gives $\sum_{i,j}\left\|\eta_{i+\frac{1}{2}}^-\right\|_{L^2(I_j^y)}^2 \leqslant Ch^{2k+1}\left\|u\right\|_{H^{k+1}(\Omega)}^2$. The y-direction is analogous, so

$$|\mathcal{H}(\eta, \xi_h)| \leqslant Ch^{k+\frac{1}{2}}\left\|u\right\|_{H^{k+1}(\Omega)} J_h(\xi_h).$$

Young's inequality and the bound on (η_t, ξ_h) give $\frac{\mathrm{d}}{\mathrm{d}t}\left\|\xi_h\right\|_{L^2(\Omega)}^2 \leqslant C\left\|\xi_h\right\|_{L^2(\Omega)}^2 + Ch^{2k+1}\widetilde{M}_T^2$. Since $\xi_h(0) = 0$, Grönwall's inequality yields $\left\|\xi_h(T)\right\|_{L^2(\Omega)} \leqslant C_T h^{k+1/2}\widetilde{M}_T$. The triangle inequality and (9) complete the proof. □

Remark 2.5. The trace inequality $\left\|\eta|_{\partial K}\right\|_{L^2(\partial K)} \lesssim h^{-1/2}\left\|\eta\right\|_{L^2(K)}$ causes the loss of half an order. The shifted projection $P_h^\star$ incorporates the DG flux into its orthogonality conditions. The residual $\mathcal{H}(u - P_h^\star u, v_h)$ is therefore expressed through differences between adjacent shifted traces rather than through individual traces. Local mesh smoothness then provides the additional factor h^θ.

2.5 Main results

We state the two main estimates under two independent structural assumptions on the nonuniform Cartesian mesh.

Locally smooth meshes. For the locally smooth mesh class, fix an exponent $\alpha > 0$ and set $\theta := \min\{\alpha, 1\}$. We call the mesh *locally smooth* if, in addition to the quasi-uniformity condition (2), there exists $C_s > 0$ independent of h such that, in the periodic sense,

$$\left|h_i^x - h_{i-1}^x\right| \leqslant C_s\, h^{1+\alpha}, \qquad \left|h_j^y - h_{j-1}^y\right| \leqslant C_s\, h^{1+\alpha}, \tag{10}$$

where $h_0^x := h_{N_x}^x$ and $h_0^y := h_{N_y}^y$. Condition (10) is stronger than shape regularity and weaker than uniformity. It provides the factor h^α in the residual estimate. The approximation order of P^k caps this gain, so $\theta = \min\{\alpha, 1\}$. For $\alpha \geqslant 1$, the estimate has the optimal order h^{k+1}.

Theorem 2.6 (L^2 estimate on locally smooth meshes)**.** *Let u be a sufficiently smooth periodic solution of (1) with*

$$u \in L^\infty(0,T;W^{k+2,\infty}(\Omega)) \cap C^1([0,T];W^{k+1,\infty}(\Omega))$$

and set

$$M_T := \sup_{0\leqslant t\leqslant T}\big(\|u(t)\|_{W^{k+2,\infty}(\Omega)} + \|u_t(t)\|_{W^{k+1,\infty}(\Omega)}\big).$$

Assume the mesh satisfies (2) and (10) with $\alpha > \frac{1}{2}$, and let $\theta = \min\{\alpha, 1\}$. Then the semidiscrete upwind DG solution satisfies

$$\|u(T) - u_h(T)\|_{L^2(\Omega)} \leqslant C_T\big(\|P_h^\star u(0) - u_h(0)\|_{L^2(\Omega)} + h^{k+\theta}M_T\big).$$

In particular, the estimate is $O(h^{k+\theta})$ if $u_h(0) = P_h^\star u(0)$ or if $u_h(0) = \mathbb{P}_h u(0)$.

Pattern-periodic meshes. We also consider a second, independent mesh class, called *pattern-periodic meshes.* Let

$$G_I^x = (X_{I-\frac{1}{2}}, X_{I+\frac{1}{2}}), \qquad G_J^y = (Y_{J-\frac{1}{2}}, Y_{J+\frac{1}{2}})$$

be a uniform macro grid with lengths H_x and H_y, where $N_X H_x = L_x$ and $N_Y H_y = L_y$, and set

$$M_{I,J} = G_I^x \times G_J^y, \qquad H = \max\{H_x, H_y\}.$$

Assume the macro rectangles are shape-regular, $c_0 \leqslant H_x/H_y \leqslant C_0$. The fixed internal pattern is specified by positive proportions

$$\alpha_1^x, \ldots, \alpha_{m_x}^x > 0, \qquad \sum_{r=1}^{m_x} \alpha_r^x = 1,$$

in the x direction and

$$\alpha_1^y, \ldots, \alpha_{m_y}^y > 0, \qquad \sum_{s=1}^{m_y} \alpha_s^y = 1,$$

in the y direction. Inside every macro cell, the fine subintervals have lengths $h_{I,r}^x = \alpha_r^x H_x$ and $h_{J,s}^y = \alpha_s^y H_y$. The fine cells are

$$K_{I,r,J,s} = I_{I,r} \times J_{J,s}.$$

The internal pattern is fixed throughout refinement; in particular m_x, m_y and

$$\alpha_{\min} := \min_{r,s}\{\alpha_r^x, \alpha_s^y\} > 0$$

are independent of h. Hence all fine cells are uniformly shape-regular and $h \simeq H$, with constants depending only on the macro aspect-ratio bounds and the fixed internal pattern.

Theorem 2.7 (Optimal estimate on pattern-periodic meshes)**.** *Assume that the mesh has the periodic structure defined above and that $k \geqslant 1$. Let $u_0 \in H^{k+2}(\Omega)$ and let u be the periodic solution of (1). If u_h solves (4) with $u_h(0) = \mathbb{P}_h u_0$, then, for every fixed $T > 0$,*

$$\|u(T) - u_h(T)\|_{L^2(\Omega)} \leqslant C_T h^{k+1} \|u_0\|_{H^{k+2}(\Omega)}.$$

The constant is independent of h, H, N_X, N_Y, but may depend on T, k and on the fixed internal pattern.

3 Error Estimates for Locally Smooth Meshes

This section proves the estimates for locally smooth meshes. We first define the shifted projection $P_h^\star$ and establish its basic properties. We then estimate the differences between shifted traces and the resulting residual. Finally, we apply Proposition 2.3 to prove Theorem 2.6.

3.1 Shifted projection: definition and properties

We now construct the local projection for P^k elements of total degree. The P^1 projection is defined by three vanishing moment conditions involving the cell and edge averages. A direct extension to P^k would be overdetermined. We therefore use a shifted upwind projection inspired by [19, §2.2.1].

Reference bilinear form. Let $\widehat{K} = [-\frac{1}{2}, \frac{1}{2}]^2$ and $\widehat{P}^k = P^k(\widehat{K})$. For $\lambda > 0$, define the reference bilinear form

$$\begin{aligned} \hat{a}_\lambda(w, z) := &- \int_{\widehat{K}} w(z_\xi + \lambda z_\eta)\, \mathrm{d}\xi\, \mathrm{d}\eta \\ &+ \int_{-1/2}^{1/2} w(\tfrac{1}{2}, \eta)\big(z(\tfrac{1}{2}, \eta) - z(-\tfrac{1}{2}, \eta)\big)\, \mathrm{d}\eta \\ &+ \lambda \int_{-1/2}^{1/2} w(\xi, \tfrac{1}{2})\big(z(\xi, \tfrac{1}{2}) - z(\xi, -\tfrac{1}{2})\big)\, \mathrm{d}\xi. \end{aligned} \tag{11}$$

This is the pullback to $\widehat{K}$ of the physical shifted upwind form, divided by h_j^y, with

$$\lambda = \frac{h_i^x}{h_j^y} \in \Lambda := \left[\tfrac{c_0}{C_0}, \tfrac{C_0}{c_0}\right].$$

We fix the monomial basis $\{\xi^\ell \eta^m : \ell + m \leqslant k+1\}$ on $\widehat{P}^{k+1}$ and denote the corresponding coefficient norm by $\|\cdot\|_{\widehat{P}^{k+1}}$. Since $\widehat{P}^{k+1}$ is finite dimensional, all polynomial norms on this space are equivalent. The constants may depend on the chosen basis, but not on h, the cell indices, or $\lambda \in \Lambda$.

Reference projection. For a continuous function ϕ, define $\widehat{P}_\lambda \phi \in \widehat{P}^k$ by

$$\int_{\widehat{K}} (\phi - \widehat{P}_\lambda \phi)\, \mathrm{d}\xi\, \mathrm{d}\eta = 0, \tag{12}$$

$$\hat{a}_\lambda(\phi - \widehat{P}_\lambda \phi, z) = 0, \qquad \forall z \in \widehat{P}^k. \tag{13}$$

When $z \equiv 1$, $z_\xi = z_\eta = 0$ and the edge differences vanish, so the constant test gives the trivial identity $0 = 0$. Thus the number of independent conditions is $1 + (\dim \widehat{P}^k - 1) = \dim \widehat{P}^k$.

Physical projection. For each $K_{i,j}$ set $\lambda_{i,j} = h_i^x / h_j^y \in \Lambda$. For a function u, denote its pullback $\hat{u}_{i,j}(\xi, \eta) = u(x_i + h_i^x \xi, y_j + h_j^y \eta)$. Define

$$(P_h^\star u)|_{K_{i,j}}(x_i + h_i^x \xi, y_j + h_j^y \eta) := \widehat{P}_{\lambda_{i,j}} \hat{u}_{i,j}(\xi, \eta). \tag{14}$$

Set $\rho = u - P_h^\star u$. On each $K_{i,j}$, $\int_{K_{i,j}} \rho \, \mathrm{d}x \, \mathrm{d}y = 0$, and for any $z \in P^k(K_{i,j})$,

$$\begin{aligned} 0 = &- \int_{K_{i,j}} \rho(z_x + z_y) \, \mathrm{d}x \, \mathrm{d}y + \int_{I_j^y} \rho(x_{i+\frac{1}{2}}, y) \big(z(x_{i+\frac{1}{2}}, y) - z(x_{i-\frac{1}{2}}, y) \big) \, \mathrm{d}y \\ &+ \int_{I_i^x} \rho(x, y_{j+\frac{1}{2}}) \big(z(x, y_{j+\frac{1}{2}}) - z(x, y_{j-\frac{1}{2}}) \big) \, \mathrm{d}x. \end{aligned} \tag{15}$$

Lemma 3.1 (Shifted projection: well-posedness and approximation)**.** *For every $\lambda \in \Lambda$ and every continuous function ϕ, $\widehat{P}_\lambda \phi$ exists and is unique. Moreover:*

(i) *If $p \in \widehat{P}^k$, then $\widehat{P}_\lambda p = p$.*

(ii) *There exists a constant C depending only on k and Λ such that*

$$\left\| \widehat{P}_\lambda \phi \right\|_{L^\infty(\widehat{K})} \leqslant C \, \|\phi\|_{L^\infty(\widehat{K})} .$$

(iii) *For all $r \in \widehat{P}^{k+1}$ and $\lambda, \mu \in \Lambda$,*

$$\left\| \widehat{P}_\lambda r - \widehat{P}_\mu r \right\|_{L^\infty(\widehat{K})} \leqslant C \, |\lambda - \mu| \; \|r\|_{\widehat{P}^{k+1}} .$$

(iv) *If $u \in W^{k+1,\infty}(K_{i,j})$, then*

$$\|u - P_h^\star u\|_{L^2(K_{i,j})} \leqslant C \, h^{k+1} \; |K_{i,j}|^{1/2} \; \|u\|_{W^{k+1,\infty}(K_{i,j})} ,$$

and therefore

$$\|u - P_h^\star u\|_{L^2(\Omega)} \leqslant C \, h^{k+1} \; \|u\|_{W^{k+1,\infty}(\Omega)} .$$

If $u \in C^1([0,T]; W^{k+1,\infty}(\Omega))$, then

$$\|(u - P_h^\star u)_t\|_{L^2(\Omega)} \leqslant C \, h^{k+1} \; \|u_t\|_{W^{k+1,\infty}(\Omega)} .$$

Proof. The proof of this lemma is postponed to Appendix A.1. □

3.2 Residual estimates for locally smooth meshes

We first recast $\mathcal{H}(\rho, v_h)$ as a sum of adjacent shifted outflow error differences, where $\rho = u - P_h^\star u$. For $v_h|_{K_{i,j}}$ we use the trace notation

$$v_{i,j}^R(y) = v_h(x_{i+\frac{1}{2}}, y)|_{K_{i,j}}, \quad v_{i,j}^L(y) = v_h(x_{i-\frac{1}{2}}, y)|_{K_{i,j}},$$

$$v_{i,j}^T(x) = v_h(x, y_{j+\frac{1}{2}})|_{K_{i,j}}, \quad v_{i,j}^B(x) = v_h(x, y_{j-\frac{1}{2}})|_{K_{i,j}},$$

and analogously $\rho_{i,j}^R$, $\rho_{i,j}^T$ are the right/top outflow traces from $K_{i,j}$.

Lemma 3.2 (Residual identity). *For every $v_h \in V_h^k$,*

$$\begin{aligned}\mathcal{H}(\rho, v_h) = &\sum_{i,j} \int_{I_j^y} \big(\rho_{i,j}^R(y) - \rho_{i-1,j}^R(y)\big) v_{i,j}^L(y)\, \mathrm{d}y \\ &+ \sum_{i,j} \int_{I_i^x} \big(\rho_{i,j}^T(x) - \rho_{i,j-1}^T(x)\big) v_{i,j}^B(x)\, \mathrm{d}x.\end{aligned} \tag{16}$$

Proof. Taking $z = v_h|_{K_{i,j}}$ in (15) gives

$$\begin{aligned}0 = &-\int_{K_{i,j}} \rho((v_h)_x + (v_h)_y)\, \mathrm{d}x\, \mathrm{d}y + \int_{I_j^y} \rho_{i,j}^R (v_{i,j}^R - v_{i,j}^L)\, \mathrm{d}y \\ &+ \int_{I_i^x} \rho_{i,j}^T (v_{i,j}^T - v_{i,j}^B)\, \mathrm{d}x.\end{aligned}$$

The corresponding cell contribution of $\mathcal{H}(\rho, v_h)$ is

$$\begin{aligned}\mathcal{H}_{i,j}(\rho, v_h) = &-\int_{K_{i,j}} \rho((v_h)_x + (v_h)_y)\, \mathrm{d}x\, \mathrm{d}y + \int_{I_j^y} \rho_{i,j}^R (v_{i,j}^R - v_{i+1,j}^L)\, \mathrm{d}y \\ &+ \int_{I_i^x} \rho_{i,j}^T (v_{i,j}^T - v_{i,j+1}^B)\, \mathrm{d}x.\end{aligned}$$

Subtracting the first identity from the second yields

$$\mathcal{H}_{i,j}(\rho, v_h) = \int_{I_j^y} \rho_{i,j}^R (v_{i,j}^L - v_{i+1,j}^L)\, \mathrm{d}y + \int_{I_i^x} \rho_{i,j}^T (v_{i,j}^B - v_{i,j+1}^B)\, \mathrm{d}x.$$

Summing over (i,j) and re-indexing periodically,

$$\sum_i \int_{I_j^y} \rho_{i,j}^R v_{i+1,j}^L\, \mathrm{d}y = \sum_i \int_{I_j^y} \rho_{i-1,j}^R v_{i,j}^L\, \mathrm{d}y,$$

and similarly in the y direction. This gives (16). □

Remark 3.3. The quantity $\rho_{i,j}^R - \rho_{i-1,j}^R$ is *not* the jump of ρ across one interface. The traces are taken from the outflow edges of adjacent cells, at $x = x_{i+\frac{1}{2}}$ and $x = x_{i-\frac{1}{2}}$. They are compared as functions on the same interval I_j^y. This difference is the basis of the shifted residual estimate.

Shifted outflow error difference estimates. The key estimate shows that, with $\theta = \min\{\alpha, 1\}$, the local smoothness condition (10) gives an extra factor h^θ in the adjacent shifted outflow error difference. When $\alpha \geqslant 1$, this recovers the additional factor of h from the uniform-mesh proof.

Reference trace error operators. Define

$$E_\lambda^R \phi(\eta) := (\phi - \widehat{P}_\lambda \phi)(\tfrac{1}{2}, \eta), \qquad E_\lambda^T \phi(\xi) := (\phi - \widehat{P}_\lambda \phi)(\xi, \tfrac{1}{2}).$$

By Lemma 3.1(i), $E_\lambda^R p = E_\lambda^T p = 0$ for $p \in \widehat{P}^k$. By Lemma 3.1(iii) restricted to boundary traces, for $r \in \widehat{P}^{k+1}$,

$$\left\|E_\lambda^R r - E_\mu^R r\right\|_{L^\infty(-1/2,1/2)} + \left\|E_\lambda^T r - E_\mu^T r\right\|_{L^\infty(-1/2,1/2)} \leqslant C\, |\lambda - \mu|\, \|r\|_{\widehat{P}^{k+1}}. \tag{17}$$

Adjacent parameter differences. From the local smoothness condition, the cell aspect ratios $\lambda_{i,j} = h_i^x/h_j^y$ satisfy

$$|\lambda_{i,j} - \lambda_{i-1,j}| \leqslant C\,h^\alpha, \qquad |\lambda_{i,j} - \lambda_{i,j-1}| \leqslant C\,h^\alpha. \tag{18}$$

For the first inequality, h_j^y is common to both ratios. Hence

$$|\lambda_{i,j} - \lambda_{i-1,j}| = \frac{|h_i^x - h_{i-1}^x|}{h_j^y} \leqslant \frac{C_s h^{1+\alpha}}{c_0 h} = \frac{C_s}{c_0}\,h^\alpha.$$

The estimate in the y direction follows in the same way, with h_i^x common to both ratios.

For the proof of the next estimate, let

$$H_{i,j}^{k+1}(\xi,\eta) := \sum_{\ell+m=k+1} \frac{\partial_x^\ell \partial_y^m u(x_i,y_j)}{\ell!m!}(h_i^x)^\ell (h_j^y)^m \xi^\ell \eta^m \in \widehat{P}^{k+1},$$

and set

$$\Delta_x H_{i,j}^{k+1} := H_{i,j}^{k+1} - H_{i-1,j}^{k+1}, \qquad \Delta_y H_{i,j}^{k+1} := H_{i,j}^{k+1} - H_{i,j-1}^{k+1}.$$

We also use the local patches

$$\omega_{i,j}^x := K_{i,j} \cup K_{i-1,j}, \qquad \omega_{i,j}^y := K_{i,j} \cup K_{i,j-1},$$

with periodic interpretation at the boundary. The local-smoothness gain enters through the leading-order decomposition

$$\rho_{i,j}^R - \rho_{i-1,j}^R = E_{\lambda_{i,j}}^R \Delta_x H_{i,j}^{k+1} + (E_{\lambda_{i,j}}^R - E_{\lambda_{i-1,j}}^R) H_{i-1,j}^{k+1} + \mathcal{O}(h^{k+2}), \tag{19}$$

as functions of the common variable $y \in I_j^y$, where the remainder is understood in $L^\infty(I_j^y)$. The Taylor coefficient comparison and the detailed proof are given in Appendix A.2.

Lemma 3.4 (Shifted trace-difference estimate)**.** *Let $\rho = u - P_h^\star u$. If $u \in W^{k+2,\infty}(\Omega)$, then*

$$\left\|\rho_{i,j}^R - \rho_{i-1,j}^R\right\|_{L^\infty(I_j^y)} \leqslant C\,h^{k+1+\theta}\,\|u\|_{W^{k+2,\infty}(\omega_{i,j}^x)}\,, \tag{20}$$

and analogously

$$\left\|\rho_{i,j}^T - \rho_{i,j-1}^T\right\|_{L^\infty(I_i^x)} \leqslant C\,h^{k+1+\theta}\,\|u\|_{W^{k+2,\infty}(\omega_{i,j}^y)}\,. \tag{21}$$

Proof. The proof of this lemma is postponed to Appendix A.2. □

Lemma 3.5 (Shifted residual estimate)**.** *Let $u \in W^{k+2,\infty}(\Omega)$ and $\rho = u - P_h^\star u$. Then for any $v_h \in V_h^k$,*

$$|\mathcal{H}(\rho, v_h)| \leqslant C\,h^{k+\theta}\,\|u\|_{W^{k+2,\infty}(\Omega)}\,\|v_h\|_{L^2(\Omega)}\,. \tag{22}$$

Proof. The proof of this lemma is postponed to Appendix A.3. □

3.3 Proof of Theorem 2.6

Proof. Set

$$\Pi_h = P_h^\star, \qquad s = k + \theta.$$

The approximation assumption (7) follows from Lemma 3.1:

$$\|u - P_h^\star u\|_{L^2(\Omega)} + \|(u - P_h^\star u)_t\|_{L^2(\Omega)} \leqslant Ch^{k+\theta} M_T,$$

because $\theta \leqslant 1$. The residual assumption (8) is Lemma 3.5:

$$|\mathcal{H}(u - P_h^\star u, v_h)| \leqslant Ch^{k+\theta} M_T \|v_h\|_{L^2(\Omega)}.$$

Thus Proposition 2.3 gives

$$\|u(T) - u_h(T)\|_{L^2(\Omega)} \leqslant C_T\big(\|P_h^\star u(0) - u_h(0)\|_{L^2(\Omega)} + h^{k+\theta} M_T\big).$$

If $u_h(0) = P_h^\star u(0)$, the initial term vanishes. If $u_h(0) = \mathbb{P}_h u(0)$, then

$$\|P_h^\star u(0) - \mathbb{P}_h u(0)\|_{L^2(\Omega)} \leqslant \|P_h^\star u(0) - u(0)\|_{L^2(\Omega)} + \|u(0) - \mathbb{P}_h u(0)\|_{L^2(\Omega)} \leqslant Ch^{k+1} M_T,$$

which is of higher order than $h^{k+\theta}$. This proves the theorem. □

Remark 3.6. When $0 < \alpha \leqslant \frac{1}{2}$, the shifted projection does not improve the baseline estimate. In this range, Proposition 2.4 gives the sharper rate $h^{k+1/2}$.

4 Error Estimates for Pattern-Periodic Meshes

This section proves the estimates for meshes with periodic patterns. Each macro cell $M_{I,J}$ is a translate of the same internal pattern. We define a local projection by identifying opposite macro edges periodically. This projection cancels the residuals on internal fine interfaces. Only terms across macro interfaces remain.

4.1 Macro-cell projection: definition and properties

For a macro cell $M = (X_L, X_R) \times (Y_B, Y_T)$, let $\mathcal{T}_h(M)$ be its internal fine partition and define

$$V_M^k := \{v \in L^2(M) : v|_K \in P^k(K),\ K \subset M\}.$$

We write

$$\Gamma_L(M) = \{X_L\} \times (Y_B, Y_T), \quad \Gamma_R(M) = \{X_R\} \times (Y_B, Y_T),$$
$$\Gamma_B(M) = (X_L, X_R) \times \{Y_B\}, \quad \Gamma_T(M) = (X_L, X_R) \times \{Y_T\}.$$

On M, the right and left macro edges and the top and bottom macro edges are identified periodically. For $q \in V_M^k$, denote the corresponding periodic traces by $q^{L,\mathrm{per}}$ and $q^{B,\mathrm{per}}$. Define the local periodic upwind form

$$\begin{aligned}
\mathcal{R}_M(z, q) := \sum_{K \subset M} -\int_K z(q_x + q_y)\,\mathrm{d}x\,\mathrm{d}y + \sum_{F \in \mathcal{F}_x^{\mathrm{int}}(M)} \int_F z^-(q^- - q^+)\,\mathrm{d}y \\
+ \sum_{F \in \mathcal{F}_y^{\mathrm{int}}(M)} \int_F z^-(q^- - q^+)\,\mathrm{d}x + \int_{\Gamma_R(M)} z^R(q^R - q^{L,\mathrm{per}})\,\mathrm{d}y \\
+ \int_{\Gamma_T(M)} z^T(q^T - q^{B,\mathrm{per}})\,\mathrm{d}x.
\end{aligned} \tag{23}$$

For a smooth function w, define $\Pi^\star_M w \in V^k_M$ by

$$(\Pi^\star_M w - w, 1)_M = 0, \qquad \mathcal{R}_M(\Pi^\star_M w - w, q) = 0, \quad \forall q \in V^k_{M,0}, \tag{24}$$

where $V^k_{M,0} := \{q \in V^k_M : (q,1)_M = 0\}$. Since $\mathcal{R}_M(z,1) = 0$, the second condition is equivalently imposed for all $q \in V^k_M$. The global macro-cell projection is

$$(I_h w)|_M = \Pi^\star_M w.$$

Lemma 4.1 (Macro-cell projection properties)**.** *Assume the internal pattern is fixed and $k \geqslant 1$. The projection $\Pi^\star_M$ exists uniquely. Moreover, for $w \in H^{k+1}(M)$,*

$$\begin{aligned} \|w - \Pi^\star_M w\|_{L^2(M)} + H \|\nabla_h(w - \Pi^\star_M w)\|_{L^2(M)} \\ + H^{1/2} \|w - \Pi^\star_M w\|_{L^2(\partial M)} \leqslant C H^{k+1} |w|_{H^{k+1}(M)}. \end{aligned} \tag{25}$$

Consequently,

$$\|w - I_h w\|_{L^2(\Omega)} \leqslant C H^{k+1} \|w\|_{H^{k+1}(\Omega)}. \tag{26}$$

For time-dependent w, $(I_h w)_t = I_h(w_t)$.

Proof. The proof of this lemma is postponed to Appendix A.4. □

4.2 Residual estimates for pattern-periodic meshes

Let $M^- = M_{I-1,J}$ and $M = M_{I,J}$. For $(x,y) \in M^-$ set

$$(\tau_x w)(x,y) = w(x + H_x, y),$$

with periodic extension. Define τ_y analogously. For $e = w - I_h w$, define the vertical macro-interface difference on $\Gamma_L(M_{I,J})$ by

$$\delta_x e = e^{R,\leftarrow}_{I,J} - e^R_{I-1,J}, \qquad e^{R,\leftarrow}_{I,J}(X_{I-\frac{1}{2}}, y) := e|_{M_{I,J}}(X_{I+\frac{1}{2}}, y).$$

Here $e^R_{I-1,J}$ is the right trace from $M_{I-1,J}$. Define $\delta_y e$ analogously on $\Gamma_B(M_{I,J})$ by shifting the top macro-edge trace of $M_{I,J}$ down by one macro length and subtracting the top trace from $M_{I,J-1}$.

Lemma 4.2 (Internal cancellation)**.** *Let w be smooth, let $\rho = w - I_h w$, and let $v_h \in V^k_h$. Then*

$$\mathcal{H}(\rho, v_h) = \sum_{I,J} \int_{\Gamma_L(M_{I,J})} \delta_x \rho \, v^L_{I,J} \, \mathrm{d}y + \sum_{I,J} \int_{\Gamma_B(M_{I,J})} \delta_y \rho \, v^B_{I,J} \, \mathrm{d}x. \tag{27}$$

Here $v^L_{I,J}$ and $v^B_{I,J}$ denote the traces of v_h from the macro cell $M_{I,J}$ on its left and bottom macro edges, respectively.

Proof. By the definition of I_h,

$$\mathcal{R}_M(\rho, v_h|_M) = 0, \qquad \forall\, M.$$

Hence we may subtract the vanishing macro-cell contributions:

$$\mathcal{H}(\rho, v_h) = \mathcal{H}(\rho, v_h) - \sum_M \mathcal{R}_M(\rho, v_h|_M).$$

The volume terms and the fine-interface terms strictly inside each macro cell are identical in the two forms. Denote by $\mathcal{H}^x, \mathcal{R}^x_M$ and $\mathcal{H}^y, \mathcal{R}^y_M$ the vertical and horizontal edge contributions of the corresponding forms. On vertical macro interfaces, the remaining terms can be re-indexed as

$$\begin{aligned}\mathcal{H}^x(\rho, v_h) - \sum_M \mathcal{R}^x_M(\rho, v_h|_M) &= \sum_{I,J} \int_{\Gamma_L(M_{I,J})} (\rho^{R,\leftarrow}_{I,J} - \rho^R_{I-1,J}) v^L_{I,J} \,\mathrm{d}y \\ &= \sum_{I,J} \int_{\Gamma_L(M_{I,J})} \delta_x \rho \, v^L_{I,J} \,\mathrm{d}y.\end{aligned}$$

The horizontal macro interfaces give, analogously,

$$\mathcal{H}^y(\rho, v_h) - \sum_M \mathcal{R}^y_M(\rho, v_h|_M) = \sum_{I,J} \int_{\Gamma_B(M_{I,J})} \delta_y \rho \, v^B_{I,J} \,\mathrm{d}x.$$

Adding the two identities gives (27). □

Lemma 4.3 (Translation covariance)**.** *Let* $\Pi^\star_M$ *denote the local macro-cell projection on* M*. On* $M^- = M_{I-1,J}$*,*

$$\Pi^\star_{M^-}(\tau_x w)(x, y) = (\Pi^\star_M w)(x + H_x, y).$$

The analogous identity holds in the y *direction.*

Proof. The shifted function on the right belongs to $V^k_{M^-}$ because the internal pattern is the same in all macro cells. After the change of variables $x \mapsto x + H_x$, it satisfies the mean condition and all equations in (24) for $\tau_x w$ on M^-. Uniqueness gives the result. □

Lemma 4.4 (Macro-interface difference estimate)**.** *If* $w \in H^{k+2}(\Omega)$ *and* $e = w - I_h w$*, then*

$$\left(\sum_{I,J} \|\delta_x e\|^2_{L^2(\Gamma_L(M_{I,J}))} + \sum_{I,J} \|\delta_y e\|^2_{L^2(\Gamma_B(M_{I,J}))} \right)^{1/2} \leqslant C H^{k+\frac{3}{2}} \|w\|_{H^{k+2}(\Omega)} . \tag{28}$$

Proof. The proof of this lemma is postponed to Appendix A.5. □

Lemma 4.5 (Pattern-periodic residual estimate)**.** *Let* $w \in H^{k+2}(\Omega)$ *and* $\rho = w - I_h w$*. Then, for all* $v_h \in V^k_h$*,*

$$|\mathcal{H}(\rho, v_h)| \leqslant C H^{k+1} \|w\|_{H^{k+2}(\Omega)} \|v_h\|_{L^2(\Omega)} . \tag{29}$$

Proof. Set

$$\begin{aligned} A^2_\rho &:= \sum_{I,J} \|\delta_x \rho\|^2_{L^2(\Gamma_L(M_{I,J}))} + \sum_{I,J} \|\delta_y \rho\|^2_{L^2(\Gamma_B(M_{I,J}))} , \\ B^2_v &:= \sum_{I,J} \left\|v^L_{I,J}\right\|^2_{L^2(\Gamma_L(M_{I,J}))} + \sum_{I,J} \left\|v^B_{I,J}\right\|^2_{L^2(\Gamma_B(M_{I,J}))} . \end{aligned}$$

By the internal cancellation identity (27) and Cauchy–Schwarz,

$$|\mathcal{H}(\rho, v_h)| \leqslant A_\rho B_v.$$

The first factor is bounded by Lemma 4.4. The second factor is controlled by the inverse trace inequality on the fixed-pattern boundary fine cells:

$$B_v \leqslant C H^{-1/2} \|v_h\|_{L^2(\Omega)} .$$

Combining these estimates gives (29). □

4.3 Proof of Theorem 2.7

Proof. For this mesh class take $\Pi_h = I_h$. By Lemma 4.1,

$$\|u - I_h u\|_{L^2(\Omega)} + \|(u - I_h u)_t\|_{L^2(\Omega)} \leqslant C H^{k+1} \|u\|_{H^{k+2}(\Omega)},$$

and by Lemma 4.5,

$$|\mathcal{H}(u - I_h u, v_h)| \leqslant C H^{k+1} \|u\|_{H^{k+2}(\Omega)} \|v_h\|_{L^2(\Omega)}.$$

Since $H \simeq h$ for a fixed internal pattern, these bounds verify the assumptions of Proposition 2.3 with $s = k+1$ and regularity measure $\sup_{0 \leqslant t \leqslant T} \|u(t)\|_{H^{k+2}(\Omega)}$. Thus Proposition 2.3 gives

$$\|u(T) - u_h(T)\|_{L^2(\Omega)} \leqslant C_T \big(\|I_h u_0 - \mathbb{P}_h u_0\|_{L^2(\Omega)} + H^{k+1} \|u_0\|_{H^{k+2}(\Omega)} \big).$$

The initial term is bounded by

$$\|I_h u_0 - \mathbb{P}_h u_0\|_{L^2(\Omega)} \leqslant \|I_h u_0 - u_0\|_{L^2(\Omega)} + \|u_0 - \mathbb{P}_h u_0\|_{L^2(\Omega)} \leqslant C H^{k+1} \|u_0\|_{H^{k+1}(\Omega)}.$$

Since $H \simeq h$ for a fixed internal pattern and the periodic transport solution preserves Sobolev norms, the desired h^{k+1} estimate follows. $\square$

5 Numerical tests

This section reports numerical tests for the transport equation in two dimensions

$$u_t + u_x + u_y = 0,$$

with the smooth periodic exact solution $u(x, y, t) = \sin(x + y - 2t)$ on $[0, 2\pi]^2$. For each mesh class, we first report the DG solution error, then use the standard local L^2 projection as a baseline, and finally test the residual mechanism central to the corresponding analysis.

For all computations of the DG solution error, the final time is $T = 1$ and the initial data are projected by the standard local L^2 projection. Time integration uses a nine-stage SSP Runge–Kutta method of ninth order for linear problems [13] and

$$\tau = \frac{0.6}{2k+1} \min\{h^x_{\min}, h^y_{\min}\}.$$

5.1 Locally smooth meshes

The locally smooth tests use nonuniform Cartesian meshes satisfying

$$|h^x_i - h^x_{i-1}| + |h^y_j - h^y_{j-1}| = O(h^{1+\alpha}),$$

with $\alpha = 0.2, 0.8, 1.0$ and four mesh levels

$$(N_x, N_y) = (42, 40), (52, 48), (62, 56), (72, 64).$$

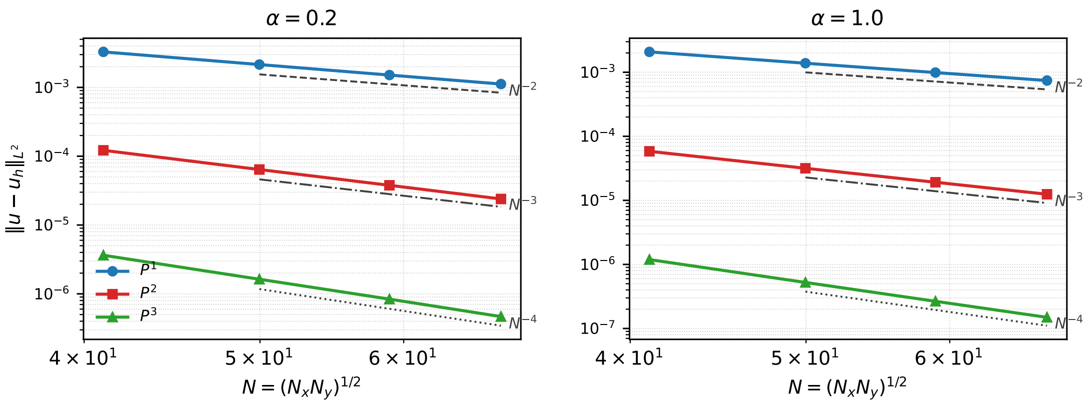

Figure 1: L^2 errors of the DG solution versus $N = (N_x N_y)^{1/2}$ for P^1, P^2, and P^3 elements on locally smooth meshes with $\alpha = 0.2$ and $\alpha = 1.0$. Reference slopes of orders two, three, and four are included for comparison.

DG solution errors. We first compute the DG solution errors on these mesh families. The cases $\alpha = 0.2$ and $\alpha = 1.0$ are shown in Figure 1, together with reference slopes of orders two, three, and four.

Baseline with the standard local L^2 projection. Let $\eta = u - \mathbb{P}_h u$ and define

$$T^x_{i,j} = \int_{I^y_j} \eta^-_{i+\frac{1}{2}}(y)[v_h]^x_{i,j}(y)\ \mathrm{d}y, \qquad T^y_{i,j} = \int_{I^x_i} \eta^-_{j+\frac{1}{2}}(x)[v_h]^y_{i,j}(x)\ \mathrm{d}x.$$

We measure the edge residual quantity

$$\frac{\sum_{i,j}\big(|T^x_{i,j}| + |T^y_{i,j}|\big)}{\|v_h\|_{\Gamma_h}}, \tag{30}$$

with

$$\|v_h\|^2_{\Gamma_h} = \sum_{i,j}\left(\int_{I^y_j} ([v_h]^x_{i,j})^2\ \mathrm{d}y + \int_{I^x_i} ([v_h]^y_{i,j})^2\ \mathrm{d}x\right).$$

On each cell, v_h is chosen by assigning deterministic pseudorandom coefficients in $[0, 1]$ to the local basis functions.

Residual associated with the mesh structure. We next use the same mesh families to examine the shifted residual, which is the central mechanism in the locally smooth analysis. To test the estimate for differences between shifted traces underlying Lemmas 3.4 and 3.5, we compute the elementwise shifted contributions

$$S^x_{i,j} = \int_{I^y_j} \big(\rho^R_{i,j}(y) - \rho^R_{i-1,j}(y)\big) v^L_{i,j}(y)\ \mathrm{d}y, \quad S^y_{i,j} = \int_{I^x_i} \big(\rho^T_{i,j}(x) - \rho^T_{i,j-1}(x)\big) v^B_{i,j}(x)\ \mathrm{d}x,$$

where $\rho = u - P^\star_h u$. On each cell, v_h is chosen as before. Table 2 reports the shifted residual quantity

$$\frac{\sum_{i,j}\big(|S^x_{i,j}| + |S^y_{i,j}|\big)}{\|v_h\|_{L^2(\Omega)}}. \tag{31}$$

Table 1: Edge residual quantity (30) for $\eta = u - \mathbb{P}_h u$ for P^k elements.

k	(N_x, N_y)	$\alpha = 0.2$		$\alpha = 0.8$		$\alpha = 1.0$	
		value	order	value	order	value	order
1	(42, 40)	3.0426×10^{-2}	–	2.6240×10^{-2}	–	2.5986×10^{-2}	–
	(52, 48)	2.2431×10^{-2}	1.540	1.9448×10^{-2}	1.513	1.9294×10^{-2}	1.504
	(62, 56)	1.7390×10^{-2}	1.542	1.5182×10^{-2}	1.501	1.5086×10^{-2}	1.491
	(72, 64)	1.3994×10^{-2}	1.535	1.2271×10^{-2}	1.504	1.2205×10^{-2}	1.497
2	(42, 40)	1.1003×10^{-3}	–	8.0327×10^{-4}	–	7.8596×10^{-4}	–
	(52, 48)	6.5445×10^{-4}	2.625	4.8336×10^{-4}	2.566	4.7511×10^{-4}	2.543
	(62, 56)	4.2606×10^{-4}	2.601	3.1861×10^{-4}	2.526	3.1420×10^{-4}	2.506
	(72, 64)	2.9437×10^{-4}	2.612	2.2244×10^{-4}	2.539	2.1987×10^{-4}	2.522
3	(42, 40)	2.3348×10^{-5}	–	1.3671×10^{-5}	–	1.3118×10^{-5}	–
	(52, 48)	1.1290×10^{-5}	3.671	6.7102×10^{-6}	3.595	6.4931×10^{-6}	3.553
	(62, 56)	6.1610×10^{-6}	3.670	3.7263×10^{-6}	3.565	3.6281×10^{-6}	3.527
	(72, 64)	3.6680×10^{-6}	3.664	2.2522×10^{-6}	3.558	2.2024×10^{-6}	3.527

Table 2: Shifted residual quantity (31) for P^k elements.

k	(N_x, N_y)	$\alpha = 0.2$		$\alpha = 0.8$		$\alpha = 1.0$	
		value	order	value	order	value	order
1	(42, 40)	6.2465×10^{-2}	–	1.8725×10^{-2}	–	1.3628×10^{-2}	–
	(52, 48)	4.8715×10^{-2}	1.256	1.3020×10^{-2}	1.836	9.1725×10^{-3}	2.000
	(62, 56)	3.9651×10^{-2}	1.247	9.6199×10^{-3}	1.834	6.5864×10^{-3}	2.007
	(72, 64)	3.3212×10^{-2}	1.252	7.4230×10^{-3}	1.832	4.9613×10^{-3}	2.002
2	(42, 40)	1.2959×10^{-3}	–	3.6356×10^{-4}	–	2.6125×10^{-4}	–
	(52, 48)	8.3378×10^{-4}	2.228	2.0938×10^{-4}	2.788	1.4546×10^{-4}	2.958
	(62, 56)	5.7748×10^{-4}	2.226	1.3220×10^{-4}	2.787	8.9348×10^{-5}	2.953
	(72, 64)	4.2103×10^{-4}	2.232	8.9025×10^{-5}	2.794	5.8697×10^{-5}	2.969
3	(42, 40)	3.5491×10^{-5}	–	1.0233×10^{-5}	–	7.0780×10^{-6}	–
	(52, 48)	1.8766×10^{-5}	3.219	4.8319×10^{-6}	3.791	3.2250×10^{-6}	3.971
	(62, 56)	1.1059×10^{-5}	3.204	2.5911×10^{-6}	3.776	1.6788×10^{-6}	3.956
	(72, 64)	7.0130×10^{-6}	3.218	1.5188×10^{-6}	3.774	9.5891×10^{-7}	3.957

Comparison of results. The DG error curves in Figure 1 display order $k+1$ in both cases shown. For $\alpha = 0.2$, the observed rate is higher than the proved rate. The standard projection residuals in Table 1 have order $k + 1/2$ and depend little on α. The shifted residuals in Table 2 have orders close to $k + 0.2$, $k + 0.8$, and $k + 1$ for $\alpha = 0.2$, 0.8, and 1.0, respectively. These results show that the shifted projection captures the additional cancellation caused by local mesh smoothness. They also confirm the predicted order $h^{k+\theta}$.

5.2 Meshes with periodic patterns

We next turn to the second mesh class and consider two fixed internal patterns. Pattern A has $m_x = 3$, $m_y = 4$, with proportions

$$(1/6, 1/2, 1/3) \quad \text{in the } x\text{-direction}, \qquad (1/5, 6/20, 7/20, 3/20) \quad \text{in the } y\text{-direction},$$

and Pattern B has $m_x = 5$, $m_y = 2$, with proportions

$$(1/5, 1/6, 2/15, 4/15, 7/30) \quad \text{in the } x\text{-direction}, \qquad (1/3, 2/3) \quad \text{in the } y\text{-direction}.$$

For the DG solution errors and the baseline based on the standard projection, we use macro resolutions $N = 8, 12, 16, 20$. The fine grid dimensions are $(3N, 4N)$ for Pattern A and $(5N, 2N)$ for Pattern B.

DG solution errors. We first compute the DG solution errors for both internal patterns. The results are shown in Figure 2, together with reference slopes of orders two, three, and four.

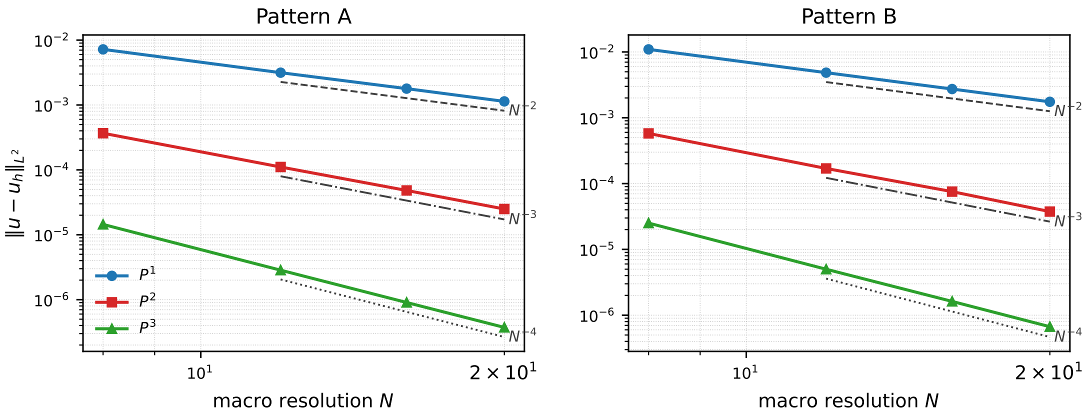

Figure 2: L^2 errors of the DG solution at $T = 1$ versus the macro resolution N for P^1, P^2, and P^3 elements on meshes with periodic patterns. Pattern A uses $(3N, 4N)$ fine cells and Pattern B uses $(5N, 2N)$ fine cells. Reference slopes of orders two, three, and four are included for comparison.

Baseline with the standard local L^2 projection. We next evaluate the edge residual quantity (30) on these meshes, using the same deterministic pseudorandom construction of v_h.

Residual associated with the mesh structure. Finally, we test the residual across macro interfaces, which is the central mechanism in the analysis of periodic patterns. For this purpose, we use the four macro grid sizes

$$(N_X, N_Y) = (42, 40), (52, 48), (62, 56), (72, 64).$$

Let $\rho = u - I_h u$, where I_h is the projection on each macro cell. Following the internal cancellation identity in Lemma 4.2, define the contributions across macro interfaces

$$R^x_{I,J} = \int_{\Gamma_L(M_{I,J})} \delta_x \rho \, v^L_{I,J} \, \mathrm{d}y, \qquad R^y_{I,J} = \int_{\Gamma_B(M_{I,J})} \delta_y \rho \, v^B_{I,J} \, \mathrm{d}x.$$

We report the absolute residual quantity across macro interfaces

$$\frac{\sum_{I,J} \left(|R^x_{I,J}| + |R^y_{I,J}| \right)}{\|v_h\|_{L^2(\Omega)}}. \tag{32}$$

Here v_h is generated by the same deterministic pseudorandom procedure.

Table 3: Edge residual quantity (30) for the standard L^2 projection on meshes with periodic patterns.

k	N	Pattern A		Pattern B	
		value	order	value	order
1	8	5.2536×10^{-2}	–	6.5740×10^{-2}	–
	12	2.8871×10^{-2}	1.476	3.5990×10^{-2}	1.486
	16	1.8682×10^{-2}	1.513	2.3374×10^{-2}	1.500
	20	1.3368×10^{-2}	1.500	1.6735×10^{-2}	1.497
2	8	2.8955×10^{-3}	–	3.4820×10^{-3}	–
	12	1.0336×10^{-3}	2.541	1.2760×10^{-3}	2.476
	16	5.0786×10^{-4}	2.470	6.2217×10^{-4}	2.497
	20	2.9099×10^{-4}	2.496	3.5572×10^{-4}	2.505
3	8	8.8011×10^{-5}	–	1.3631×10^{-4}	–
	12	2.1166×10^{-5}	3.515	3.3113×10^{-5}	3.490
	16	7.7332×10^{-6}	3.500	1.2108×10^{-5}	3.497
	20	3.5498×10^{-6}	3.489	5.5515×10^{-6}	3.495

Table 4: Residual quantity (32) across macro interfaces for P^k elements and two internal patterns.

k	(N_X, N_Y)	Pattern A		Pattern B	
		value	order	value	order
1	$(42, 40)$	5.9442×10^{-4}	–	7.5045×10^{-4}	–
	$(52, 48)$	3.9728×10^{-4}	1.887	5.0408×10^{-4}	2.183
	$(62, 56)$	2.8927×10^{-4}	1.804	3.6353×10^{-4}	2.120
	$(72, 64)$	2.1744×10^{-4}	1.909	2.7890×10^{-4}	1.985
2	$(42, 40)$	7.5527×10^{-6}	–	1.5561×10^{-5}	–
	$(52, 48)$	3.5930×10^{-6}	3.478	8.9312×10^{-6}	3.045
	$(62, 56)$	2.0316×10^{-6}	3.242	5.3607×10^{-6}	3.311
	$(72, 64)$	1.2686×10^{-6}	3.149	3.3911×10^{-6}	3.430
3	$(42, 40)$	3.6390×10^{-8}	–	1.3663×10^{-7}	–
	$(52, 48)$	1.5301×10^{-8}	4.057	5.3050×10^{-8}	5.189
	$(62, 56)$	7.8008×10^{-9}	3.830	2.6523×10^{-8}	4.497
	$(72, 64)$	4.4008×10^{-9}	3.828	1.4962×10^{-8}	4.288

Comparison of results. The DG solution errors in Figure 2 approach orders two, three, and four for P^1, P^2, and P^3, respectively. Both patterns give the same orders. The standard projection residuals in Table 3 have only order $k + 1/2$. In contrast, the residuals across macro interfaces in Table 4 have order $k+1$, as predicted by Lemma 4.5. The internal pattern affects the constants and the values before the asymptotic regime, but not the asymptotic order. These results support the cancellation mechanism at the macro scale.

6 Conclusion

We have analyzed the semidiscrete upwind DG method with P^k elements of total degree on two classes of structured nonuniform Cartesian meshes. A common framework based on projection errors reduces both analyses to approximation and residual estimates.

1. For locally smooth meshes, the shifted projection converts the residual into differences between adjacent outflow errors. Variation in the cell aspect ratios gives the rate $h^{k+\theta}$, where $\theta = \min\{\alpha, 1\}$. For $\alpha \leqslant \frac{1}{2}$, the standard projection gives the sharper bound $h^{k+1/2}$.

2. For meshes with periodic patterns, translation at the macro scale cancels the residuals on internal fine interfaces. The remaining terms across macro interfaces have order h^{k+1} because $H \simeq h$.

These results show that convergence on nonuniform Cartesian meshes depends on both shape regularity and the structure of the interface projection mismatch. Local smoothness gives an approximate shifting mechanism. A periodic pattern gives an exact mechanism at the macro scale. The analysis may be extended to fully discrete Runge–Kutta schemes and equations with variable coefficients. Nonlinear equations and more general meshes are also of interest.

A Proofs of the lemmas

This appendix collects the proofs of the lemmas stated in the body of the paper. As an additional consistency check, selected lemmas and theorems in the analysis were formally verified using the Lean interactive theorem prover [11].

A.1 Proof of Lemma 3.1

Homogeneous uniqueness.

If $k = 0$, w is a constant and the integral condition forces $w = 0$. Assume $k \geqslant 1$ and take $z = w$. A direct computation gives

$$\hat{a}_\lambda(w, w) = \tfrac{1}{2} \int_{-1/2}^{1/2} \big(w(\tfrac{1}{2}, \eta) - w(-\tfrac{1}{2}, \eta)\big)^2 \,\mathrm{d}\eta + \tfrac{\lambda}{2} \int_{-1/2}^{1/2} \big(w(\xi, \tfrac{1}{2}) - w(\xi, -\tfrac{1}{2})\big)^2 \,\mathrm{d}\xi.$$

Since $\lambda > 0$ and $\hat{a}_\lambda(w, w) = 0$,

$$w(\tfrac{1}{2}, \eta) = w(-\tfrac{1}{2}, \eta), \qquad w(\xi, \tfrac{1}{2}) = w(\xi, -\tfrac{1}{2}).$$

Integrating by parts on z with these equal traces, all shifted boundary contributions cancel and

$$\hat{a}_\lambda(w, z) = \int_{\widehat{K}} (w_\xi + \lambda w_\eta)\, z \,\mathrm{d}\xi \;\mathrm{d}\eta.$$

Taking $z = w_\xi + \lambda w_\eta \in \widehat{P}^{k-1} \subset \widehat{P}^k$ gives $w_\xi + \lambda w_\eta = 0$. Hence $w(\xi, \eta) = F(\eta - \lambda\xi)$ for a univariate polynomial F of degree at most k.

Set $t = \eta - \lambda/2$. The equality of the traces gives $F(t) = F(t + \lambda)$ for all $t \in \mathbb{R}$. Suppose that $\deg F = m \geqslant 1$ and that its leading coefficient is $a_m \neq 0$. Then $G(t) := F(t + \lambda) - F(t)$ has leading coefficient $m a_m \lambda \neq 0$ at degree $m - 1$. This contradicts $G \equiv 0$. Therefore F and w are constant. The integral condition then gives $w \equiv 0$.

Well-posedness and reference estimates.

Choose a basis $\{\psi_0 = 1, \psi_1, \dots, \psi_{N-1}\}$ of $\widehat{P}^k$ with $N = \dim \widehat{P}^k$, and write $\widehat{P}_\lambda \phi = \sum_m c_m \psi_m$. The system (12)–(13) becomes $A(\lambda)\, c = b(\lambda, \phi)$, where

$$A_{\ell m}(\lambda) = \begin{cases} \int_{\widehat{K}} \psi_m, & \ell = 0, \\ \hat{a}_\lambda(\psi_m, \psi_\ell), & \ell = 1, \dots, N-1, \end{cases} \qquad b_\ell(\lambda, \phi) = \begin{cases} \int_{\widehat{K}} \phi, & \ell = 0, \\ \hat{a}_\lambda(\phi, \psi_\ell), & \ell = 1, \dots, N-1. \end{cases}$$

Existence and uniqueness. If $A(\lambda)\, c = 0$, the polynomial $w = \sum_m c_m \psi_m \in \widehat{P}^k$ satisfies $\int_{\widehat{K}} w = 0$ and $\hat{a}_\lambda(w, \psi_\ell) = 0$ for $\ell \geqslant 1$. Since $\hat{a}_\lambda(w, 1) = 0$ holds automatically, $\hat{a}_\lambda(w, z) = 0$ for all $z \in \widehat{P}^k$. By the homogeneous uniqueness just proved, $w \equiv 0$, hence $c = 0$. Thus $A(\lambda)$ is non-singular.

Property (i). If $p \in \widehat{P}^k$, then $w := p - \widehat{P}_\lambda p$ satisfies the homogeneous conditions; by homogeneous uniqueness, $w = 0$.

Property (ii). Each entry of $A(\lambda)$ is affine in λ, so A is continuous on Λ. The matrix is nonsingular for every $\lambda \in \Lambda$, and Λ is compact. Therefore $\det A$ has a positive lower bound on Λ. It follows that $A(\lambda)^{-1} = \operatorname{adj} A(\lambda) / \det A(\lambda)$ is uniformly bounded:

$$\sup_{\lambda \in \Lambda} \left\| A(\lambda)^{-1} \right\| < \infty.$$

The test functions ψ_ℓ are fixed. Hence the right-hand side satisfies

$$\left| \int_{\widehat{K}} \phi \right| + \sum_\ell |\hat{a}_\lambda(\phi, \psi_\ell)| \leqslant C \, \|\phi\|_{L^\infty(\widehat{K})}$$

uniformly for $\lambda \in \Lambda$. Thus $\|c\| \leqslant C \, \|\phi\|_{L^\infty(\widehat{K})}$. Norm equivalence on the finite dimensional space proves (ii).

Property (iii). Because A is affine in λ and $r \in \widehat{P}^{k+1}$ is fixed,

$$\|A(\lambda) - A(\mu)\| \leqslant C \, |\lambda - \mu| \,, \qquad \|b(\lambda, r) - b(\mu, r)\| \leqslant C \, |\lambda - \mu| \; \|r\|_{\widehat{P}^{k+1}} \,.$$

The identity $A(\lambda)^{-1} - A(\mu)^{-1} = A(\lambda)^{-1} \big(A(\mu) - A(\lambda) \big) A(\mu)^{-1}$ combined with the uniform bound on $\|A^{-1}\|$ gives $\|A(\lambda)^{-1} - A(\mu)^{-1}\| \leqslant C \, |\lambda - \mu|$. Writing

$$c(\lambda) - c(\mu) = A(\lambda)^{-1} \big(b(\lambda, r) - b(\mu, r) \big) + \big(A(\lambda)^{-1} - A(\mu)^{-1} \big) b(\mu, r)$$

and using $\|b(\mu, r)\| \leqslant C \, \|r\|_{\widehat{P}^{k+1}}$, we obtain

$$\|c(\lambda) - c(\mu)\| \leqslant C \, |\lambda - \mu| \; \|r\|_{\widehat{P}^{k+1}} \,,$$

and norm equivalence yields (iii).

Physical approximation estimates. On each $K_{i,j}$, let $T^k_{i,j} u \in P^k(K_{i,j})$ be the kth-order Taylor polynomial of u at (x_i, y_j). By Lemma 3.1(i), $P^\star_h T^k_{i,j} u = T^k_{i,j} u$, hence

$$u - P^\star_h u = (I - P^\star_h)(u - T^k_{i,j} u).$$

Taylor's theorem gives $\left\| u - T^k_{i,j} u \right\|_{L^\infty(K_{i,j})} \leqslant C \, h^{k+1} \, \|u\|_{W^{k+1,\infty}(K_{i,j})}$. By Lemma 3.1(ii) and affine scaling, $\left\| P^\star_h (u - T^k_{i,j} u) \right\|_{L^\infty(K_{i,j})} \leqslant C \, \left\| u - T^k_{i,j} u \right\|_{L^\infty(K_{i,j})}$, so

$$\|u - P^\star_h u\|_{L^\infty(K_{i,j})} \leqslant C \, h^{k+1} \, \|u\|_{W^{k+1,\infty}(K_{i,j})} \,.$$

Multiplying by $|K_{i,j}|^{1/2}$ gives the local L^2 estimate, and summing over cells gives the global one.

For the time derivative, since the mesh is fixed in time, $\lambda_{i,j}$ and the system matrix $A(\lambda_{i,j})$ are time-independent. Under $u \in C^1([0,T]; W^{k+1,\infty})$, the volume and edge integrals defining the projection are differentiable in t and differentiation commutes with the linear projection conditions, giving $\partial_t(P_h^\star u) = P_h^\star u_t$. Applying the spatial estimate to u_t completes the proof.

A.2 Proof of Lemma 3.4

Leading Taylor coefficient comparison.

We first prove the x-direction coefficient estimate. For each $\ell + m = k+1$, compare the coefficients

$$C_{i,j}^{\ell,m} = \tfrac{(h_i^x)^\ell (h_j^y)^m}{\ell! m!} \, \partial_x^\ell \partial_y^m u(x_i, y_j), \quad C_{i-1,j}^{\ell,m} = \tfrac{(h_{i-1}^x)^\ell (h_j^y)^m}{\ell! m!} \, \partial_x^\ell \partial_y^m u(x_{i-1}, y_j).$$

Add and subtract $\partial_x^\ell \partial_y^m u(x_{i-1}, y_j)(h_i^x)^\ell (h_j^y)^m$ to split the difference into

$$C_{i,j}^{\ell,m} - C_{i-1,j}^{\ell,m} = \text{(I)} + \text{(II)},$$

where

$$\begin{aligned} \text{(I)} &= \tfrac{(h_i^x)^\ell (h_j^y)^m}{\ell! m!} \big(\partial_x^\ell \partial_y^m u(x_i, y_j) - \partial_x^\ell \partial_y^m u(x_{i-1}, y_j) \big), \\ \text{(II)} &= \tfrac{\partial_x^\ell \partial_y^m u(x_{i-1}, y_j)}{\ell! m!} \big((h_i^x)^\ell - (h_{i-1}^x)^\ell \big) (h_j^y)^m. \end{aligned}$$

For (I), since $\ell + m = k+1$,

$$\begin{aligned} &\left| \partial_x^\ell \partial_y^m u(x_i, y_j) - \partial_x^\ell \partial_y^m u(x_{i-1}, y_j) \right| \leqslant Ch \, \|u\|_{W^{k+2,\infty}(\omega_{i,j}^x)}, \\ &(h_i^x)^\ell (h_j^y)^m \leqslant Ch^{k+1}. \end{aligned}$$

Consequently,

$$|\text{(I)}| \leqslant Ch^{k+2} \|u\|_{W^{k+2,\infty}(\omega_{i,j}^x)} \leqslant Ch^{k+1+\theta} \|u\|_{W^{k+2,\infty}(\omega_{i,j}^x)},$$

where we used $\theta \leqslant 1$.

For (II), if $\ell \geqslant 1$, the local smoothness condition gives

$$\left| (h_i^x)^\ell - (h_{i-1}^x)^\ell \right| \leqslant Ch^{\ell-1} \left| h_i^x - h_{i-1}^x \right| \leqslant Ch^{\ell+\alpha}.$$

Together with $(h_j^y)^m \leqslant Ch^m$, this gives

$$|\text{(II)}| \leqslant Ch^{k+1+\alpha} \|u\|_{W^{k+1,\infty}(K_{i-1,j})} \leqslant Ch^{k+1+\theta} \|u\|_{W^{k+2,\infty}(\omega_{i,j}^x)}.$$

If $\ell = 0$, term (II) vanishes. In either case,

$$\left| C_{i,j}^{\ell,m} - C_{i-1,j}^{\ell,m} \right| \leqslant Ch^{k+1+\theta} \|u\|_{W^{k+2,\infty}(\omega_{i,j}^x)}.$$

Taking the maximum over the finitely many (ℓ, m) with $\ell + m = k+1$ gives

$$\left\| \Delta_x H_{i,j}^{k+1} \right\|_{\widehat{P}^{k+1}} \leqslant Ch^{k+1+\theta} \|u\|_{W^{k+2,\infty}(\omega_{i,j}^x)}. \tag{33}$$

At a periodic boundary (e.g., comparing $i=1$ with $i=N_x$), extend u periodically to $\mathbb{R}^2$, interpret $x_0 = x_{N_x} - L_x$ and $K_{0,j} = K_{N_x,j} - L_x\hat{x}$; then $|x_1 - x_0| = O(h)$ and $h_0^x = h_{N_x}^x$, so the estimate is unchanged. The y direction gives

$$\left\|\Delta_y H_{i,j}^{k+1}\right\|_{\widehat{P}^{k+1}} \leqslant Ch^{k+1+\theta} \|u\|_{W^{k+2,\infty}(\omega_{i,j}^y)}. \tag{34}$$

Shifted trace-difference estimate. We prove (20); the proof of (21) is identical. On the reference cell of $K_{i,j}$,

$$\hat{u}_{i,j} = T_{i,j}^k + H_{i,j}^{k+1} + R_{i,j}^{k+2}, \qquad \left\|R_{i,j}^{k+2}\right\|_{L^\infty(\widehat{K})} \leqslant Ch^{k+2} \|u\|_{W^{k+2,\infty}(K_{i,j})}.$$

Since $E_\lambda^R p = 0$ for $p \in \widehat{P}^k$,

$$\rho_{i,j}^R(y_j + h_j^y \eta) = E_{\lambda_{i,j}}^R H_{i,j}^{k+1}(\eta) + E_{\lambda_{i,j}}^R R_{i,j}^{k+2}(\eta). \tag{35}$$

The same formula holds on $K_{i-1,j}$. Therefore, as functions of the common variable $y = y_j + h_j^y \eta$,

$$\begin{aligned}\rho_{i,j}^R - \rho_{i-1,j}^R = {} & E_{\lambda_{i,j}}^R (H_{i,j}^{k+1} - H_{i-1,j}^{k+1}) \\ & + (E_{\lambda_{i,j}}^R - E_{\lambda_{i-1,j}}^R) H_{i-1,j}^{k+1} + \mathcal{O}(h^{k+2}).\end{aligned}$$

The first term satisfies

$$\left\|E_{\lambda_{i,j}}^R (H_{i,j}^{k+1} - H_{i-1,j}^{k+1})\right\|_{L^\infty(-1/2,1/2)} \leqslant C \left\|\Delta_x H_{i,j}^{k+1}\right\|_{\widehat{P}^{k+1}} \leqslant Ch^{k+1+\theta} \|u\|_{W^{k+2,\infty}(\omega_{i,j}^x)}.$$

For the second term, by (17) and (18),

$$\begin{aligned}&\left\|(E_{\lambda_{i,j}}^R - E_{\lambda_{i-1,j}}^R) H_{i-1,j}^{k+1}\right\|_{L^\infty(-1/2,1/2)} \\ &\quad \leqslant C|\lambda_{i,j} - \lambda_{i-1,j}| \left\|H_{i-1,j}^{k+1}\right\|_{\widehat{P}^{k+1}} \leqslant Ch^\alpha h^{k+1} \|u\|_{W^{k+1,\infty}(K_{i-1,j})} \\ &\quad \leqslant Ch^{k+1+\theta} \|u\|_{W^{k+2,\infty}(\omega_{i,j}^x)}.\end{aligned}$$

The two remainder terms are controlled by the boundary stability of E_λ^R and the Taylor remainder estimate:

$$\left\|E_{\lambda_{i,j}}^R R_{i,j}^{k+2}\right\|_{L^\infty(-1/2,1/2)} + \left\|E_{\lambda_{i-1,j}}^R R_{i-1,j}^{k+2}\right\|_{L^\infty(-1/2,1/2)} \leqslant Ch^{k+2} \|u\|_{W^{k+2,\infty}(\omega_{i,j}^x)}.$$

Since $\theta \leqslant 1$, this is bounded by $Ch^{k+1+\theta} \|u\|_{W^{k+2,\infty}(\omega_{i,j}^x)}$. This proves (20).

A.3 Proof of Lemma 3.5

By Lemma 3.2, $\mathcal{H}(\rho, v_h) = S_x + S_y$, with

$$S_x = \sum_{i,j} \int_{I_j^y} \Delta_{i,j}^x(y) v_{i,j}^L(y)\, \mathrm{d}y, \quad \Delta_{i,j}^x := \rho_{i,j}^R - \rho_{i-1,j}^R,$$

and analogously S_y with $\Delta_{i,j}^y = \rho_{i,j}^T - \rho_{i,j-1}^T$.

For S_x, Lemma 3.4 gives

$$\left\|\Delta_{i,j}^x\right\|_{L^2(I_j^y)} \leqslant Ch^{k+1+\theta} (h_j^y)^{1/2} \|u\|_{W^{k+2,\infty}(\omega_{i,j}^x)}.$$

Applying Cauchy–Schwarz cell by cell and inserting the weight $(h_i^x)^{1/2}$,

$$
\begin{aligned}
|S_x| &\leqslant \sum_{i,j} \left\|\Delta_{i,j}^x\right\|_{L^2(I_j^y)} \left\|v_{i,j}^L\right\|_{L^2(I_j^y)} \\
&\leqslant \left(\sum_{i,j} \frac{\left\|\Delta_{i,j}^x\right\|_{L^2(I_j^y)}^2}{h_i^x}\right)^{1/2} \left(\sum_{i,j} h_i^x \left\|v_{i,j}^L\right\|_{L^2(I_j^y)}^2\right)^{1/2}.
\end{aligned}
$$

The trace inverse inequality on $\widehat{K}$ gives

$$
\left\|p(-\tfrac{1}{2},\cdot)\right\|_{L^2(-1/2,1/2)}^2 \leqslant C\, \|p\|_{L^2(\widehat{K})}^2, \qquad p \in \widehat{P}^k.
$$

After affine scaling,

$$
h_i^x \left\|v_{i,j}^L\right\|_{L^2(I_j^y)}^2 \leqslant C\, \|v_h\|_{L^2(K_{i,j})}^2, \qquad h_j^y \left\|v_{i,j}^B\right\|_{L^2(I_i^x)}^2 \leqslant C\, \|v_h\|_{L^2(K_{i,j})}^2.
$$

Therefore

$$
\sum_{i,j} h_i^x \left\|v_{i,j}^L\right\|_{L^2(I_j^y)}^2 \leqslant C\, \|v_h\|_{L^2(\Omega)}^2.
$$

For the first factor, quasi-uniformity gives

$$
\frac{\left\|\Delta_{i,j}^x\right\|_{L^2(I_j^y)}^2}{h_i^x} \leqslant C h^{2k+2+2\theta}\, \|u\|_{W^{k+2,\infty}(\Omega)}^2.
$$

Since $N_x N_y \leqslant C h^{-2}$, the first factor is bounded by $C h^{k+\theta}\, \|u\|_{W^{k+2,\infty}(\Omega)}$. Hence

$$
|S_x| \leqslant C h^{k+\theta}\, \|u\|_{W^{k+2,\infty}(\Omega)}\, \|v_h\|_{L^2(\Omega)}.
$$

The estimate for S_y is analogous. Combining the two estimates gives (22).

A.4 Proof of Lemma 4.1

For any $p \in V_M^k$, the local periodic energy identity reads

$$
\begin{aligned}
\mathcal{R}_M(p,p) = {}& \frac{1}{2} \sum_{F \in \mathcal{F}_x^{\mathrm{int}}(M)} \int_F (p^- - p^+)^2 \,\mathrm{d}y + \frac{1}{2} \sum_{F \in \mathcal{F}_y^{\mathrm{int}}(M)} \int_F (p^- - p^+)^2 \,\mathrm{d}x \\
&+ \frac{1}{2} \int_{\Gamma_R(M)} (p^R - p^{L,\mathrm{per}})^2 \,\mathrm{d}y + \frac{1}{2} \int_{\Gamma_T(M)} (p^T - p^{B,\mathrm{per}})^2 \,\mathrm{d}x.
\end{aligned}
\tag{36}
$$

For the homogeneous problem, taking $q = p$ gives

$$
\mathcal{R}_M(p,p) = 0 \quad \Longrightarrow \quad [p] = 0 \text{ on all local periodic interfaces.}
$$

Hence p is continuous on the locally periodic macro cell, and

$$
\mathcal{R}_M(p,q) = (p_x + p_y, q)_M, \qquad q \in V_{M,0}^k.
$$

Moreover,

$$
(p_x + p_y, 1)_M = \int_{\partial M} p(n_x + n_y) \,\mathrm{d}\sigma = 0,
$$

where the last equality uses the local periodicity on opposite macro edges. Thus $p_x+p_y \in V^k_{M,0}$, and choosing $q = p_x + p_y$ yields

$$\|p_x + p_y\|^2_{L^2(M)} = 0 \quad \Longrightarrow \quad p_x + p_y = 0.$$

Thus, on each fine cell K, there is a one-variable polynomial F_K such that

$$p(x, y) = F_K(y - x), \qquad (x, y) \in K.$$

Across a common vertical or horizontal fine edge, the traces of p agree. Along such an edge, the variable $s = y - x$ ranges over a nonempty interval, so the corresponding one-variable polynomials agree on an interval and are identical. By connectivity of the fine partition, all F_K coincide with one polynomial F. The right-left local periodicity gives

$$F(s - H_x) = F(s)$$

on a nonempty interval, hence everywhere as a polynomial identity. Since $H_x > 0$, F is constant; hence p is constant, and

$$(p, 1)_M = 0 \quad \Longrightarrow \quad p = 0.$$

The homogeneous solution is therefore trivial, so the finite-dimensional system defining $\Pi^\star_M$ is nonsingular.

Mapping M to the reference macro cell gives a fixed internal pattern and a normalized matrix $A(\lambda_M)$, where $\lambda_M = H_x/H_y \in [c_0, C_0]$. The preceding uniqueness implies

$$\det A(\lambda_M) \neq 0, \qquad \lambda_M \in [c_0, C_0],$$

and compactness gives

$$\sup_{\lambda_M \in [c_0, C_0]} \left\| A(\lambda_M)^{-1} \right\| < \infty.$$

Define

$$\mathcal{N}_M(z) := \|z\|_{L^2(M)} + H \|\nabla_h z\|_{L^2(M)} + H^{1/2} \|z\|_{L^2(\partial M)}.$$

After scaling back to M,

$$\mathcal{N}_M(\Pi^\star_M z) \leqslant C \mathcal{N}_M(z).$$

Since $\Pi^\star_M p = p$ for $p \in V^k_M$,

$$\mathcal{N}_M(w - \Pi^\star_M w) \leqslant C \inf_{p \in V^k_M} \mathcal{N}_M(w - p) \leqslant C H^{k+1} |w|_{H^{k+1}(M)},$$

which is (25). Summing over macro cells gives (26). Since the mesh is fixed in time, $\partial_t(I_h w) = I_h(w_t)$.

A.5 Proof of Lemma 4.4

We prove the x estimate. On $M^- = M_{I-1,J}$ define

$$\mathcal{E}^-_R(\phi) = (\phi - \Pi^\star_{M^-}\phi)|_{\Gamma_R(M^-)}.$$

By linearity of the projection and Lemma 4.3, the shifted interface difference satisfies, after identifying $\Gamma_L(M)$ with $\Gamma_R(M^-)$,

$$\delta_x e = \mathcal{E}_R^-(\tau_x w) - \mathcal{E}_R^-(w) = \mathcal{E}_R^-(\tau_x w - w).$$

The boundary part of (25) gives

$$\|\delta_x e\|_{L^2(\Gamma_L(M))} = \left\|\mathcal{E}_R^-(\tau_x w - w)\right\|_{L^2(\Gamma_R(M^-))} \leqslant CH^{k+\frac{1}{2}}|\tau_x w - w|_{H^{k+1}(M^-)}.$$

For $|\beta| = k+1$,

$$D^\beta(\tau_x w - w)(x,y) = \int_0^{H_x} \partial_x D^\beta w(x+s,y)\,\mathrm{d}s,$$

so $|\tau_x w - w|_{H^{k+1}(M^-)} \leqslant CH_x \|w\|_{H^{k+2}(M^- \cup_x M)}$. This yields the local bound $CH^{k+3/2}$ on each macro interface. Squaring and summing gives (28), because neighboring macro patches overlap uniformly. The y direction is identical.

Declaration of Generative AI Use

The authors used ChatGPT (OpenAI) during the preparation of this manuscript to improve the clarity and readability of the English writing and to assist with language editing. All AI-assisted revisions were carefully reviewed, verified, and edited by the authors, who take full responsibility for the content of the manuscript.

References

[1] W. Cao, C.-W. Shu, Y. Yang, and Z. Zhang, Superconvergence of discontinuous Galerkin method for 2-D hyperbolic equations, *SIAM J. Numer. Anal.* **53** (2015), 1651–1671.

[2] W. Cao, C.-W. Shu, and Z. Zhang, Unified analysis of the semidiscrete discontinuous Galerkin methods for 2-D hyperbolic equations on Cartesian meshes using P^k elements: optimal error estimates and superconvergence, *Math. Comp.* **95** (2026), 1225–1250.

[3] Y. Cheng and C.-W. Shu, Superconvergence and time evolution of discontinuous Galerkin finite element solutions, *J. Comput. Phys.* **227** (2008), 9612–9627.

[4] P.G. Ciarlet, The finite element method for elliptic problems, *North-Holland*, Amsterdam, 1978.

[5] B. Cockburn, B. Dong, and J. Guzmán, Optimal convergence of the original DG method for the transport-reaction equation on special meshes, *SIAM J. Numer. Anal.* **46** (2008), 1250–1265.

[6] B. Cockburn, S. Hou, and C.-W. Shu, The Runge–Kutta local projection discontinuous Galerkin finite element method for conservation laws IV. The multidimensional case, *Math. Comp.* **54** (1990), 545–581.

[7] B. Cockburn and C.-W. Shu, TVB Runge–Kutta local projection discontinuous Galerkin finite element method for conservation laws II: General framework, *Math. Comp.* **52** (1989), 411–435.

[8] B. Cockburn and C.-W. Shu, The Runge–Kutta local projection P^1-discontinuous Galerkin finite element method for scalar conservation laws, *RAIRO Modél. Math. Anal. Numér.* **25** (1991), 337–361.

[9] B. Cockburn and C.-W. Shu, The local discontinuous Galerkin method for time-dependent convection-diffusion systems, *SIAM J. Numer. Anal.* **35** (1998), 2440–2465.

[10] B. Cockburn and C.-W. Shu, The Runge–Kutta discontinuous Galerkin method for conservation laws V: Multidimensional systems, *J. Comput. Phys.* **141** (1998), 199–224.

[11] L. de Moura and S. Ullrich, The Lean 4 theorem prover and programming language, in *Automated Deduction—CADE 28*, Lecture Notes in Computer Science, vol. 12699, Springer, Cham, 2021, pp. 625–635.

[12] R.S. Falk and G.R. Richter, Explicit finite element methods for symmetric hyperbolic equations, *SIAM J. Numer. Anal.* **36** (1999), 935–952.

[13] S. Gottlieb, C.-W. Shu, and E. Tadmor, Strong stability-preserving high-order time discretization methods, *SIAM Rev.* **43** (2001), 89–112.

[14] P. Houston, C. Schwab, and E. Süli, Stabilized *hp* finite element methods for first-order hyperbolic problems, *SIAM J. Numer. Anal.* **37** (2000), 1618–1643.

[15] C. Johnson and J. Pitkäranta, An analysis of the discontinuous Galerkin method for a scalar hyperbolic equation, *Math. Comp.* **46** (1986), 1–26.

[16] P. LeSaint and P.A. Raviart, On a finite element method for solving the neutron transport equation, in *Mathematical Aspects of Finite Elements in Partial Differential Equations* (C. de Boor, ed.), Academic Press, 1974, pp. 89–145.

[17] Q. Lin, N. Yan, and A. Zhou, An optimal error estimate of the discontinuous Galerkin method, *Gongcheng Shuxue Xuebao* **13** (1996), 101–105.

[18] Y. Liu, C.-W. Shu, and M. Zhang, Optimal error estimates of the semidiscrete central discontinuous Galerkin methods for linear hyperbolic equations, *SIAM J. Numer. Anal.* **56** (2018), 520–541.

[19] Y. Liu, C.-W. Shu, and M. Zhang, Optimal error estimates of the semidiscrete discontinuous Galerkin methods for two dimensional hyperbolic equations on Cartesian meshes using P^k elements, *ESAIM: M2AN* **54** (2020), 705–726.

[20] X. Meng, C.-W. Shu, and B. Wu, Optimal error estimates for discontinuous Galerkin methods based on upwind-biased fluxes for linear hyperbolic equations, *Math. Comp.* **85** (2016), 1225–1261.

[21] A. Naga and Z. Zhang, A posteriori error estimates based on the polynomial preserving recovery, *SIAM J. Numer. Anal.* **42** (2004), 1780–1800.

[22] T. Peterson, A note on the convergence of the discontinuous Galerkin method for a scalar hyperbolic equation, *SIAM J. Numer. Anal.* **28** (1991), 133–140.

[23] W.H. Reed and T.R. Hill, Triangular mesh methods for the neutron transport equation, *Los Alamos Scientific Laboratory report LA-UR-73-479*, 1973.

[24] G.R. Richter, An optimal-order error estimate for the discontinuous Galerkin method, *Math. Comp.* **50** (1988), 75–88.

[25] Y. Xu and C.-W. Shu, Optimal error estimates of the semidiscrete local discontinuous Galerkin methods for high order wave equations, *SIAM J. Numer. Anal.* **50** (2012), 79–104.

[26] J. Xu and Z. Zhang, Analysis of recovery type a posteriori error estimators for mildly structured grids, *Math. Comp.* **73** (2004), 1139–1152.

[27] Y. Yang and C.-W. Shu, Analysis of optimal superconvergence of discontinuous Galerkin method for linear hyperbolic equations, *SIAM J. Numer. Anal.* **50** (2012), 3110–3133.

[28] Q. Zhang and C.-W. Shu, Error estimates to smooth solutions of Runge–Kutta discontinuous Galerkin methods for scalar conservation laws, *SIAM J. Numer. Anal.* **42** (2004), 641–666.

[29] A. Zhou and Q. Lin, Optimal and superconvergence estimates of the finite element method for a scalar hyperbolic equation, *Acta Math. Sci.* **14** (1994), 90–94.